Boundary element method for electron transport in the presence of pointlike scatterers in magnetic fields

Tsuyoshi Ueta*
Department of Applied Physics, Faculty of Engineering, Chiba University, 1-33 Yayoi-cho, Inage-ku, Chiba 263-8522, Japan
(Received 13 October 1998; revised manuscript received 20 April 1999)

The boundary element method for electron waves in the presence of uniform magnetic fields is extended so that it is applicable to scattering problems by many scatterers. The cross sections of scatterers are assumed to be so small that the scattering potentials are modeled by summation of δ functions. This extended method is applied to a magnetic electron focusing geometry with a sequence of scatterers between an emitter and a collector. The transmission probability of an electron wave from the emitter to the collector is computed as a function of the magnetic field. Electron distributions are also calculated. These evidently show the commensurate scattering classically expected. The results of sample calculations demonstrate the effectiveness of the method. [S0163-1829(99)01235-7]

I. INTRODUCTION

Since magnetoresistance anomalies were experimentally observed in two-dimensional (2D) electron systems with an array of stationary scatterers (an antidot array) fabricated on an interface of the $GaAs/Al_xGa_{1-x}As$ heterostructure,[1–4] the transport of 2D electrons in such systems has been rigorously studied also theoretically. In the theoretical treatment, a potential of the form

$$V(x,y)=V_0\left[\cos\left(\frac{\pi}{a}x\right)\cos\left(\frac{\pi}{a}y\right)\right]^{2\beta}$$

(where a is the lattice constant and β is the control parameter of the steepness of the antidots) or the periodically arranged well potential of finite or infinite height are usually employed in order to model an antidot array.[5] Then, mostly infinite systems without boundaries or with periodic boundary conditions are considered and magnetoresistivity by making use of Kubo's linear-response theory or band structures are computed.[6,7] Few works for the electron systems confined in cavities have been reported. For the case that a few obstacles exist within the system surrounded by arbitrary-shaped boundaries, certainly the boundary element method for electron waves in magnetic fields[8] is applicable by modeling the scattering potentials by well potentials of finite or infinite height. We, then, need to take more than four nodes on the boundaries of the scattering potentials and at each node two unknown variables (a wave function and its normal derivative) are assigned. When a lot of scatterers exist, the number of the matrix elements of the discretized integral equation, memory space required on a computer, and cpu time becomes too large. Thus, it seems that such a method is not practicable. In this paper, an approximate solution practical for the system with many obstacles of small cross sections is presented.

For the systems with scattering potentials, the 2D volume integral of the product of the potential, the wave function, and the Green's function appears in the expression of the wave function within the region surrounded by a closed boundary. Here we consider the scatterers of small cross sections, so that the 2D volume integration is approximately evaluated. Then, we take a node in order to evaluate the volume integral for a scatterer. The method developed here is applied to a magnetic electron focusing geometry[9] with a sequence of scatterers between an emitter and a collector (Fig. 1). The result is physically interpreted and discussed.

II. BOUNDARY INTEGRAL EQUATION

The x and y axes are defined in the plane as shown in Fig. 1 and the vector potential which generates a uniform magnetic field perpendicular to the plane $\mathbf{B}=(0,0,-B)$ is defined as $\mathbf{A}(\mathbf{r})(\nabla\times\mathbf{A}=\mathbf{B})$.

The Schrödinger equation of an electron moving in the influence of the magnetic field and a scalar potential $V(\mathbf{r})$ is generally written in a dimensionless form as

$$\left[\frac{1}{2}[-i\nabla-\mathbf{A}(\mathbf{r})]^2+V(\mathbf{r})\right]\psi(\mathbf{r})=\varepsilon\psi(\mathbf{r}), \qquad (2.1)$$

where length and energy are scaled by the magnetic length $l_B\equiv\sqrt{\hbar/|qB|}$ and by the cyclotron energy $\hbar\omega_c$ ($\omega_c=|qB|/m^*$), respectively. The quantities q and m^* denote the electron charge and the effective mass in semiconductors. The scaled total wave number is defined by $K\equiv\sqrt{2\varepsilon}$.

By means of the Green's function[10,11]

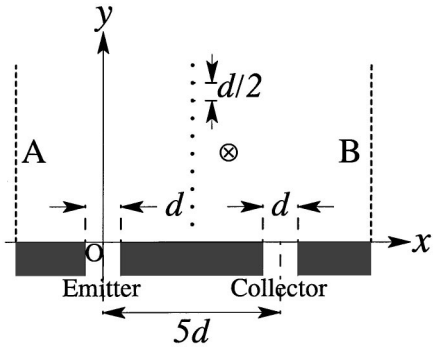

FIG. 1. Magnetic electron focusing geometry and the definition of the coordinate system.

$$G(\mathbf{r},\mathbf{r}';\varepsilon)=\exp\left[i\mathcal{S}\int_{\mathbf{r}'}^{\mathbf{r}}\mathbf{A}(\mathbf{r}'')\cdot d\mathbf{r}''\right]G_0(z;\varepsilon),$$

$$G_0(z;\varepsilon)\equiv\frac{1}{4\pi}\Gamma(\tfrac{1}{2}-\varepsilon)U(\tfrac{1}{2}-\varepsilon,1,z)\exp(-z/2), \quad (2.2)$$

which satisfies

$$\frac{1}{2}[i\nabla'-\mathbf{A}(\mathbf{r}')]^2G(\mathbf{r},\mathbf{r}';\varepsilon)=\varepsilon G(\mathbf{r},\mathbf{r}';\varepsilon)+\delta(\mathbf{r}-\mathbf{r}'), \quad (2.3)$$

we can express the wave function within the region surrounded by the closed boundary S in terms of the integral along the boundary,

$$\begin{aligned}\psi(\mathbf{r})=&\oint[G(\mathbf{r},\mathbf{r}';\varepsilon)\nabla'\psi(\mathbf{r}')\\&-\psi(\mathbf{r}')\nabla'G(\mathbf{r},\mathbf{r}';\varepsilon)]\cdot\mathbf{n}'dS'\\&-2i\oint G(\mathbf{r},\mathbf{r}';\varepsilon)\psi(\mathbf{r}')\mathbf{A}(\mathbf{r}')\cdot\mathbf{n}'dS'\\&-2\int G(\mathbf{r},\mathbf{r}';\varepsilon)\psi(\mathbf{r}')V(\mathbf{r}')d\mathbf{r}', \quad (2.4)\end{aligned}$$

where $\mathbf{n}'$ is the unit normal vector directed outwards from the region. Here, $z=(\mathbf{r}-\mathbf{r}')^2/2$ and $U(\frac{1}{2}-\varepsilon,1,z)$ is a logarithmic solution of Kummer's functions.[12] The S in front of the integral of Eq. (2.2) implies that the path of the line integral connects the point $\mathbf{r}'$ and $\mathbf{r}$ straightly. Concerning the last term on the right-hand side, we must perform the volume integral.

By moving point $\mathbf{r}$ on the boundary S, the integral equation can be constructed as follows:

$$c(\mathbf{r})\psi(\mathbf{r})=\psi_0(\mathbf{r})-2\int G(\mathbf{r},\mathbf{r}';\varepsilon)\psi(\mathbf{r}')V(\mathbf{r}')d\mathbf{r}',$$

$$\psi_0(\mathbf{r})\equiv\mathrm{P}\oint dS'\left(G(\mathbf{r},\mathbf{r}')\frac{\partial\psi(\mathbf{r}')}{\partial n'}-\psi(\mathbf{r}')\frac{\partial G(\mathbf{r},\mathbf{r}')}{\partial n'}-2iG(\mathbf{r},\mathbf{r}')\psi(\mathbf{r}')\mathbf{A}(\mathbf{r}')\cdot\mathbf{n}'\right), \quad (2.5)$$

where the symbol ''P'' and $\partial/\partial n'$ denotes the Cauchy's principal value of the integral and outward-normal derivative, respectively. The coefficient $c(\mathbf{r})$ comes from the volume integration $\int d\mathbf{r}'$ of the delta function $\delta(\mathbf{r}-\mathbf{r}')$, which is not unity since $\mathbf{r}$ lies on the boundary S. If the boundary curve has a corner with internal angle $\theta(\mathbf{r})$ at $\mathbf{r}$, then $c(\mathbf{r})=\theta(\mathbf{r})/2\pi$.[13] Obviously, $c(\mathbf{r})=1/2$ if the boundary on point $\mathbf{r}$ is smooth.

III. APPROXIMATION

Let us consider N_s scatterers of the same scattering amplitude and cross section. The potential of a scatterer is modeled by a cylindrical barrier of finite height V and radius a, so that the total potential is written as

$$V(\mathbf{r})=\overline{Va^2}\frac{1}{2}(Kd)^2\sum_{n=1}^{N_s}\frac{1}{\pi a^2}\theta(a-|\mathbf{r}-\mathbf{R}_n|), \quad (3.1)$$

where $\overline{V}$ and $\overline{a}$ are defined by $\overline{V}\equiv V/\varepsilon=V/(\frac{1}{2}K^2)$ and $\overline{a}\equiv a/d$. The function $\theta(x)$ denotes the unit step function. The quantities ε $(\equiv\frac{1}{2}K^2)$ and d are the energy of the incident electrons and the width of orifices (the emitter and the collector), respectively. The position vector of the center of nth scatterer is expressed by $\mathbf{R}_n$. We can take $\mathbf{R}_n$'s arbitrarily. We make the radius a small enough keeping $\overline{Va^2}$ constant, since scatterers of small cross section are considered. The scattering potential $(1/\pi a^2)\theta(a-|\mathbf{r}-\mathbf{R}_n|)$ may, then, be approximated by Dirac's δ function $\delta(\mathbf{r}-\mathbf{R}_n)$. We can immediately evaluate the 2D volume integration in Eq. (2.5) and obtain

$$c(\mathbf{r})\psi(\mathbf{r})=\psi_0(\mathbf{r})-\overline{Va^2}(Kd)^2\sum_{n=1}^{N_s}G(\mathbf{r},\mathbf{R}_n)\psi(\mathbf{R}_n). \quad (3.2)$$

In Eq. (3.2), $\psi(\mathbf{R}_n)$'s are unknown variables to be determined. If $\mathbf{r}$ is set on $\mathbf{R}_m$ $(1\leqslant m\leqslant N_s)$ [then $c(\mathbf{R}_m)=1$ since $\mathbf{R}_m$ is a internal point], $G(\mathbf{R}_m,\mathbf{R}_m)$ in the summation is divergent. Originally, such divergence does not occur, so that when we take $\mathbf{r}$ as $\mathbf{R}_m$, we need to evaluate the volume integration, including the potential whose center is located at $\mathbf{R}_m$,

$$\frac{1}{\pi a^2}\int G(\mathbf{R}_m,\mathbf{r}')\theta(a-|\mathbf{r}'-\mathbf{R}_m|)\psi(\mathbf{r}')d\mathbf{r}',$$

more accurately in order to avoid the divergence.

Now, considering the small scattering radius a, we may reasonably estimate as

$$\exp\left[i\mathcal{S}\int_{\mathbf{r}'}^{\mathbf{R}_m}\mathbf{A}(\mathbf{r}'')\cdot d\mathbf{r}''\right]\sim 1,$$

$$\exp(-z/2)\sim 1,$$

and obtain the expansion of the Kummer function $U(\frac{1}{2}-\varepsilon,1,z)$ for small z,[12]

$$\Gamma(\tfrac{1}{2}-\varepsilon)U(\tfrac{1}{2}-\varepsilon,1,z)\sim-[\ln z+\Psi(\tfrac{1}{2}-\varepsilon)-2\gamma].$$

Here, $\Psi(\frac{1}{2}-\varepsilon)$ and γ are the digamma function and Euler's constant, respectively. Within the range in which the scattering potential has a finite (nonzero) value, the wave function $\psi(\mathbf{r})$ in the integrand should not vary very far from the value at the center $\mathbf{R}_m$, so that we may write $\psi(\mathbf{r})\sim\psi(\mathbf{R}_m)$. In this approximation, the wave function in the integrand is independent of the position, and it can be taken outside the integral. Finally, we obtain

$$\frac{1}{\pi a^2}\int G(\mathbf{R}_m,\mathbf{r}')\,\theta(a-|\mathbf{r}'-\mathbf{R}_m|)\,\psi(\mathbf{r}')\,d\mathbf{r}'$$

$$\sim -\frac{1}{\pi a^2}\,\frac{\psi(\mathbf{R}_m)}{4\pi}\int \theta(a-|\mathbf{r}'-\mathbf{R}_m|)$$

$$\times[\ln z+\Psi(\tfrac{1}{2}-\varepsilon)-2\gamma]\,d\mathbf{r}'$$

$$=-\frac{\psi(\mathbf{R}_m)}{4\pi}\left[\ln\frac{a^2}{2}-1+\Psi(\tfrac{1}{2}-\varepsilon)-2\gamma\right]. \quad (3.3)$$

Therefore, when $\mathbf{r}$ is taken as $\mathbf{R}_m$ in Eq. (2.5), $G(\mathbf{R}_m,\mathbf{R}_m)$ is replaced by $-(1/4\pi)[\kappa+\Psi(\frac{1}{2}-\varepsilon)]$ with $\kappa\equiv\ln(a^2/2)-1-2\gamma=\ln\frac{1}{2}(\overline{ad})^2-1-2\gamma$.

IV. APPLICATION

As an example of application, this extended method is applied to a magnetic electron focusing geometry with scatterers (Fig. 1). The scatterers lie on the middle line between the emitter and the collector at intervals of $d/2$, that is, their positions are given by $(x,y)=(d/2)(5,n)$ (n is a natural number).

In the absence of a magnetic field, when the boundaries A and B (Fig. 1) are located enough in the distance from both orifices of the emitter and the collector, the integration on the portion A and B on the right-hand side of Eq. (2.4) need not be performed owing to the Sommerfeld radiation condition. In the presence of a magnetic field, however, this condition does not hold.

In classical mechanics, electrons in magnetic fields move on cyclotron orbits. In our system, electrons injected from the emitter travel toward the virtual boundary B along the wall, repeating the fractional cyclotron motion, whose radius is $r_c\equiv K=\sqrt{2\varepsilon}$, and collision with the wall and with the scatterers. Therefore, electrons never go away farther than $2r_c$ from the wall and scatterers. Quantum mechanically, the wave functions show rapid (Gaussian) decay and will not have a significant amplitude in the distance farther than $2r_c$ from the wall and the obstacles. Such behavior of wave functions is confirmed by the fact that the Green's function $G(\mathbf{r},\mathbf{r}';\varepsilon)$ falls rapidly when $|\mathbf{r}-\mathbf{r}'|$ is larger than the cyclotron diameter $2r_c$.

The electron waves propagate toward the boundary B along the wall, so that it seems that the integration along the boundary A on the right-hand side of Eq. (2.5) need not be performed. However, this is not valid at all. Time-reversal symmetry of electron motion is broken in an external magnetic field. That appears in the fact that $G_0(z;\varepsilon)$ is real. Namely, we cannot impose the outgoing (or incoming) wave condition on the Green's function in contrast to the case in the absence of a magnetic field. Therefore, solutions of Eq. (2.5) include waves coming in from the boundary A and flowing out to the emitter unless the integration along the boundary A is performed with an outgoing wave condition.

The confinement potential at the walls is assumed to be infinitely high. On the wall, the wave function $\psi(\mathbf{r}')$ vanishes, so that only the first term is left on the right-hand side of the second equation of Eq. (2.5). Its normal derivative $\partial\psi/\partial n'$ is unknown.

Edge states are formed when electrons are confined in a waveguide subjected to magnetic fields.[14,15] Although wave functions at the orifices should, then, be expanded in terms of the edge states, the influence of magnetic fields will be small when the cyclotron diameter is sufficiently larger than the width of the waveguides as we will consider now. So we put $\mathbf{A}(\mathbf{r})=\mathbf{0}$ within the emitter and the collector, that is, in the region of $y<0$. It is, then, convenient to employ the Landau gauge $\mathbf{A}=(-y,0,0)$, since the vector potential must be continuous even on the x axis.

When an electron wave belonging to the transverse mode α is injected, the total wave function in the emitter of width d is written as

$$\psi_\alpha(\mathbf{r})=u_\alpha^*(\mathbf{r})+\sum_\beta r_{\alpha\beta}\;u_\beta(\mathbf{r}),$$

$$u_\alpha(\mathbf{r})\equiv\exp(-ik_{y,\alpha}y)\sqrt{\frac{2}{d}}\sin\left[k_{x,\alpha}\left(x+\frac{d}{2}\right)\right],$$

$$k_{x,\alpha}\equiv\alpha\pi/d,\quad k_{y,\alpha}=\sqrt{K^2-k_{x,\alpha}^2} \quad (4.1)$$

$$(\alpha,\beta=1,2,\ldots).$$

On the orifice of the emitter, the reflection coefficients $r_{\alpha\beta}$ are unknown variables.

The wave function in the collector of width d is, then, expressed as

$$\psi_\alpha(\mathbf{r})=\sum_\lambda t_{\alpha\lambda}\;w_\lambda(\mathbf{r}),$$

$$w_\lambda(\mathbf{r})\equiv\exp(-ik_{y,\lambda}y)\sqrt{\frac{2}{d}}\sin\left[k_{x,\lambda}\left(x+\frac{d}{2}-L\right)\right], \quad (4.2)$$

where L is the interval between the centers of the emitter and the collector which is taken as $L=5d$ in the present paper. On the orifice of the collector, the transmission coefficients $t_{\alpha\beta}$ are unknown variables.

On the boundaries A and B, the wave functions are expanded in terms of the edge states $\chi(\mathbf{r},\kappa_\beta)$ as[15]

$$\psi_\alpha(\mathbf{r})=\sum_\gamma s_{\alpha\gamma}\;\chi(\mathbf{r},\kappa_\gamma) \quad (4.3)$$

and

$$\psi_\alpha(\mathbf{r})=\sum_\delta u_{\alpha\delta}\;\chi(\mathbf{r},\kappa_\delta), \quad (4.4)$$

respectively. Here, the edge states are defined by

$$\chi(\mathbf{r},\kappa)\equiv\exp(i\kappa x)\;\;\varphi(y,\kappa), \quad (4.5)$$

where $\varphi(y,\kappa)$'s are eigenstates of the differential equation

$$\left[-\frac{d^2}{dy^2}+(\kappa+y)^2\right]\varphi(y,\kappa)=2\varepsilon\varphi(y,\kappa) \quad (4.6)$$

with boundary conditions that $\varphi(y,\kappa)$ vanishes on the potential walls and in the distance from the walls. The wave numbers κ_γ and κ_δ are selected so that Eqs. (4.3) and (4.4) will

express outgoing waves on boundaries A and B. The coefficients $s_{\alpha\gamma}$, $u_{\alpha\delta}$ are other unknown variables to be determined. Here, note that the eigen-wave-vector κ for large enough ε has complex values as Schult *et al.*[15] pointed out.

The discretization and the numerical implementation are performed according to the usual procedure of the boundary element method in terms of the first-order (linear) elements. The general and detail formulation process of the equations can be found from Ref. 11 and existing textbooks. In the discretization scheme, nodes defined on the walls are concentrated in the region where rapid spatial variation of the wave functions is expected. The set of linear equations obtained by the discretization is solved for the unknown variables, $\partial\psi_i/\partial n'$, $r_{\alpha,\beta}$, $s_{\alpha,\delta}$, $t_{\alpha,\lambda}$, $u_{\alpha,\sigma}$, and $\psi(\mathbf{R}_n)$. Substituting the obtained values of these into Eq. (2.5), we obtain the value of the wave functions within the region surrounded by the boundary.

In experiments, the conductance between the emitter and the collector is obtained. It is well known that the conductance is proportional to the summation of the transmission probability for all of the injected propagating modes. In our formulation, we can evaluate the transmission probability of electrons from the emitter to the collector by means of the Landauer-Büttiker formula.[9] When the αth propagating mode is injected, it is given by

$$T_\alpha = \sum_{\beta=1}^{N_F} \frac{v_\beta}{v_\alpha} |t_{\alpha\beta}|^2, \tag{4.7}$$

where v_α and v_β are the group velocities of electrons belonging to the αth mode in the emitter and to the βth mode in the collector, respectively. The number N_F denotes the maximum index of propagating modes in each waveguide.

V. NUMERICAL RESULTS

We introduce a dimensionless parameter $\tilde{B}=B/B_0$ for the magnetic induction (magnetic flux density), with $B_0 \equiv \hbar/qd^2$. When the width of the emitter is, for example, 250 nm, the magnetic induction corresponding to $\tilde{B}=1$ is about 0.01 T. Throughout the present paper, we employ $Kd=15\sqrt{2}$. Then, six modes can propagate within the emitter and the collector, that is, $N_F=6$. This is an example of such a short wavelength that it is hard to analyze it by means of the other numerical methods. The parameters of the scattering potential $\overline{V}$ and $\overline{a}$ are taken as $\overline{V}=300$ and $\overline{a}=0.1$. The coefficient of the scattering potential is obtained as $\overline{Va^2}(Kd)^2=1350$.

In the practical computation, the total number of nodes is 390 including the nodes of the scatterers. The number of the scatterers N_s is 20. The maximum value of β in Eq. (4.1) and λ in Eq. (4.2) is set to 40. The number of the propagating modes in the emitter and the collector is equal to 6, so that a lot of evanescent modes are included in the expansions. The upper limit of δ and σ is taken to be the number of the propagating modes, since the amplitudes of the evanescent modes converge to very small values if the boundaries A and B are located in the distance from the orifice of the emitter and that of the collector, respectively.

The magnetic-field dependence of T_α [magnetic electron focusing spectrum (EFS)] was calculated for the injection of the fundamental mode ($\alpha=1$). The result is shown in Fig. 2 by the solid line. EFS in the absence of the scatterers is also shown by the dashed line. Substructures are observed as well as periodic major peaks. The lth major peak appears when the electron beam focuses on the collector after $l-1$ times reflection from the potential walls. The width of the major peaks in Fig. 2 increases with l. This is because classical electrons move within a finite width of a beam.[16] The series of subpeaks between $\tilde{B}=10$ and $\tilde{B}=15$ reflects the periodic arrangement of the scatterers. The positions of the subpeaks agree with values of the magnetic field at which the electron beam of width d propagating along the classical trajectory collides with the scatterers.

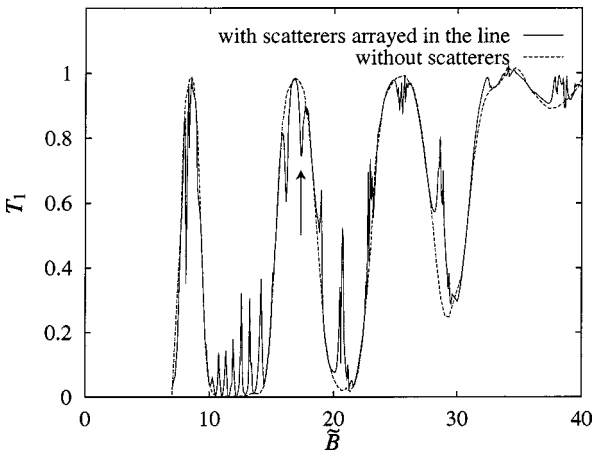

FIG. 2. Magnetic-field dependence of the transmission probability from the emitter to the collector for the fundamental mode injection T_1, which in the absence of the scatterers is also shown by the dashed line. $Kd=15\sqrt{2}$ is employed as an example of a short wavelength.

At some of the subpeaks and of the subdips, the cyclotron diameter is equal to an integral multiple of the interval between scatterers, that is, $2r_c=2\hbar K/qB=2d(Kd)/\tilde{B}=n\times d/2$ (n is a natural number). Characteristic trajectories satisfying such a commensurate condition are called ''runaway orbits.'' Electrons can, then, travel along the series of the scatterers owing to sequential collisions with the scatterers. In order to confirm that, a contour of electron density $|\psi(\mathbf{r})|^2$ is presented in Fig. 3 for $\tilde{B}=17.3333$ where $2r_c/(d/2)=4Kd/\tilde{B}\sim 5$. The value of $\tilde{B}$ is indicated by an arrow in Fig. 2. Here, the contours are assigned in the range which includes all interesting parts of the plot. We see that the probability density is distributed along the series of the scatterers. The wave function on the right-hand side of the line of the scatterers consists of the component passing through the scatterers and that going to the end of the series and turning back by successive collisions, for the number of the scatterers taken into consideration, $N_s=20$ is finite. The electron density distributions on the other commensurate conditions (that is, different values of n) also show similar behavior. It is obvious that the classical picture is effective when the incident wave of $Kd=15\sqrt{2}$ belongs to the fundamental mode.

In this case, we chose as $Kd=15\sqrt{2}$ and $\overline{a}=0.1$. Then,

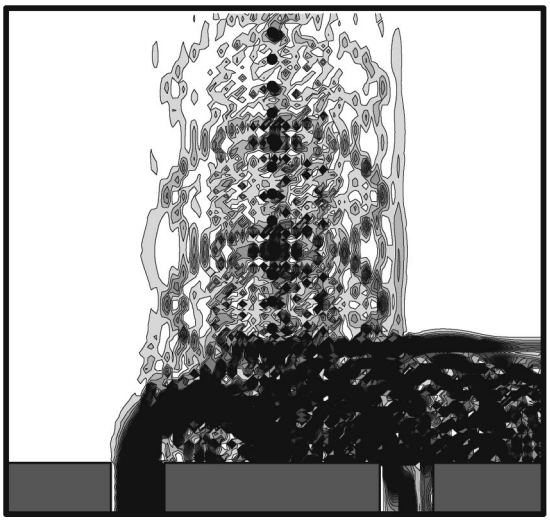

FIG. 3. Contour of the density of the electrons of Fig. 2 at $\tilde{B} = 17.3333$. The value of $\tilde{B}$ is pointed out in Fig. 2 by an arrow.

the ratio of the radius a of the scattering potential to the wavelength λ becomes

$$\frac{2\pi}{\lambda}a = Ka = Kd \cdot \overline{a} = 15\sqrt{2} \cdot 0.1 \sim 2.1.$$

The diameter $2a$ is larger than half of the wavelength, so that an electron wave may be scattered by the scatterer. In fact, the scattering amplitude becomes extremely small if $\overline{a}$ is taken smaller than 0.1.

Conservation of probability (unitarity) is employed in order to rate the accuracy of the numerical calculation. The accuracy of conservation of probability is of the order of 10^{-2}% for most cases and better than a few percent even for all cases, when $\tilde{B}$ is larger than 8.5. (When $\tilde{B}$ is smaller than 8.5, the accuracy becomes worse remarkably, since the Green's function oscillates very rapidly.[11]) Thus, we see that the approximation in Sec. III scarcely affects the accuracy.

On the other hand, even if the accuracy of conservation of probability is about 10^{-2}%, we have physically strange cases where the probability density around the collector is unusually large. This will be caused by truncating the sum with an infinite upper limit of Eq. (4.2), for the wave function has a very fine structure due to scattering, so that the coefficients of the higher modes in the collector will not be small enough. The accuracy of the conservation is not influenced because only the coefficients of the evanescent modes which do not transport current are incorrect.

VI. SUMMARY AND DISCUSSIONS

The boundary element method for 2D electron systems in uniform magnetic fields have been extended so that it is applicable to 2D electron systems with many small obstacles. As an example, it has been applied to a magnetic focusing geometry with scatterers lined up on the middle line between the emitter and the collector. The density distribution and the magnetic-field dependence of the transmission probability from the emitter to the collector (EFS) have been calculated. Then, if the diameter of the scattering potential is larger than one-half of the wavelength, the electron wave has been scattered in spite of the approximation of the scattering potential by a δ function. This method enables us to analyze 2D electron systems with more than 20 obstacles with sufficient accuracy in a feasible cpu time. It is applicable only to obstacles of small scattering cross sections. Nonetheless, it is powerful to analyze systems with a number of small obstacles.

In the last several years, many laboratories have achieved the preparation of periodic nanostructure in semiconductor heterojunctions and measured magnetoresistance, the Hall effect, and far infrared with square, rectangular, triangular, quasiperiodic, and random lattices. The results show many peculiarities. Some of them cannot be explained by using a billiard model of reflecting disks and are considered as quantum-mechanical effects. Therefore, we anticipate a practical application of the method developed here to such problems. In addition, we can easily treat the obstacles by means of this method, so that it may possibly enable us to determine the positions of the obstacles in a 2D electron system by measuring the conductance or the magnetoresistance.

*Electronic address: ueta@j90.tg.chiba-u.ac.jp

[1] D. Weiss, M. L. Roukes, A. Menschig, P. Grambow, K. von Klitzing, and G. Weimann, Phys. Rev. Lett. **66**, 2790 (1991).
[2] D. Weiss, K. Richter, A. Menschig, R. Bergmann, H. Schweizer, K. von Klitzing, and G. Weiman, Phys. Rev. Lett. **70**, 4118 (1993).
[3] F. Nihey, S. W. Hwang, and K. Nakamura, Phys. Rev. B **51**, 4649 (1995).
[4] R. Schuster, K. Ensslin, J. P. Kotthaus, G. Böhm, and W. Klein, Phys. Rev. B **55**, 2237 (1997).
[5] R. Fleischmann, T. Geisel, and R. Ketzmerick, Phys. Rev. Lett. **68**, 1367 (1992).
[6] S. Ishizaka, F. Nihey, K. Nakamura, J. Sone, and T. Ando, Phys. Rev. B **51**, 9881 (1995).
[7] T. Nagao, J. Phys. Soc. Jpn. **65**, 2606 (1996).
[8] T. Ueta, Eng. Anal. Boundary Elem. **17**, 69 (1996).
[9] H. van Houten, C. W. J. Beenakker, J. G. Williamson, M. E. I. Broekaart, and P. H. M. van Loosdrecht, Phys. Rev. B **39**, 8556 (1989).
[10] V. V. Dodonov, I. A. Malkin, and V. I. Man'ko, Phys. Lett. **51A**, 133 (1975).
[11] T. Ueta, J. Phys. Soc. Jpn. **61**, 4314 (1992).
[12] *Handbook of Mathematical Functions*, edited by M. Abramowitz and I. A. Stegun (Dover, New York, 1970), pp. 504–515.
[13] C. A. Brebbia, *The Boundary Element Method for Engineers* (Pentech, London, 1978).
[14] F. M. Peeters, Phys. Rev. Lett. **61**, 589 (1988).
[15] R. L. Schult, H. W. Wyld, and D. G. Ravenhall, Phys. Rev. B **41**, 12 760 (1990).
[16] T. Ueta, J. Phys. Soc. Jpn. **64**, 4813 (1995).